Inorganic Chemistry
Article

Inorg. Chem. **2009**, *48*, 10769–10779 **10769**
DOI: 10.1021/ic901177c

Titanium(IV) Complexes with *N,N′*-Dialkyl-2,3-dihydroxyterephthalamides and 1-Hydroxy-2(1*H*)-pyridinone as Siderophore and Tunichrome Analogues

Ritika Uppal, Hayley P. Israel, Christopher D. Incarvito, and Ann M. Valentine*

Department of Chemistry, Yale University, P.O. Box 208107, New Haven, Connecticut 06520-8107

Received June 22, 2009

The aqueous chemistry of Ti(IV) with biological ligands siderophores and tunichromes is modeled by using *N,N′*-dialkyl-2,3-dihydroxyterephthalamides (alTAMs), analogues of catecholamide-containing biomolecules, and 1-hydroxy-2(1*H*)-pyridinone (1,2-HOPO), an analogue of hydroxamate-containing biomolecules. Both types of ligands stabilize Ti(IV) with respect to hydrolytic precipitation, and afford tractable complexes. Complexes with the methyl derivative of alTAM, meTAM, are characterized by using mass spectrometry and UV/vis spectroscopy. Complexes with etTAM are characterized by the same techniques as well as X-ray crystallography, cyclic voltammetry, and spectropotentiomeric titration. The ESI mass spectra of these complexes in water show both 1:2 and 1:3 metal/ligand species. The X-ray crystal structure of a 1:2 complex, $K_2[Ti(etTAM)_2(OCH_3)_2]\cdot 2CH_3OH$ (**1**), is reported. The midpoint potential for reduction of **1** dissolved in solution is −0.98 V. A structure for a 1:3 Ti/etTAM species, $Na_2[Ti(etTAM)_3]$ demonstrates the coordination and connectivity in that complex. Spectropotentiometric titrations in water reveal three metal-containing species in solution between pH 3 and 10. 1,2-HOPO supports Ti(IV) complexes that are stable and soluble in aqueous solution. The bis-HOPO complex $[Ti(1,2\text{-}HOPO)_2(OCH_3)_2]$ (**5**) was characterized by X-ray crystallography and by mass spectrometry in solution, and the tris-HOPO dimer $[(1,2\text{-}HOPO)_3TiOTi(1,2\text{-}HOPO)_3]$ (**6**) was characterized by X-ray crystallography. Taken together, these experiments explore the characteristics of complexes that may form between siderophores and tunichromes with Ti(IV) in biology and in the environment, and guide efforts toward new, well characterized aqueous Ti(IV) complexes. By revealing the identities and some characteristics of complexes that form under a variety of conditions, these studies further our understanding of the complicated nature of aqueous titanium coordination chemistry.

Introduction

Catecholamide and hydroxamate moieties are common in biomolecules associated with metal chelation such as siderophores[1−5] and tunichromes (Chart 1).[6,7] These are ligands or potential ligands for hard Lewis acidic metals that are otherwise prone to hydrolysis and insolubility in aqueous solution at neutral pH.

Siderophores containing catecholamides (such as enterobactin) and hydroxamates (such as desferrioxamine B) are produced by bacteria to solubilize and sequester Fe(III) under aerobic conditions, making that ion bioavailable.[1−5] The tightest complex of Fe(III) is formed with enterobactin (log $K \sim 52$).[8] This value reflects the inherently tight binding of the catechol moiety,[9] reinforced by the chelate effect. The stability constant for the binding of the tris-hydroxamate desferrioxamine B to Fe(III) is log $K \sim 31$.[9] Siderophores also have medicinal applications. They have been used for the removal of excess iron from the body, in MRI contrast agents, and as siderophore-antibiotic conjugates for the treatment of drug-resistant microbes.[1]

Tunichromes (such as Mm-1 and Mm-2) are derivatized peptides containing 3,4-dihydroxyphenylalanine (DOPA) moieties isolated from ascidian blood cells.[10] Ascidians are marine invertebrate chordates, filter feeders that are commonly known as sea squirts.[11] Some species

*To whom correspondence should be addressed. E-mail: ann.valentine@yale.edu.

(1) Raymond, K. N.; Muller, G.; Matzanke, B. F. *Top. Curr. Chem.* **1984**, *123*, 49–102.
(2) Crichton, R. R.; Charloteaux-Wauters, M. *Eur. J. Biochem.* **1987**, *164*, 485–506.
(3) Albrecht-Gary, A. M.; Crumbliss, A. L. The Coordination Chemistry of Siderophores: Thermodynamics and Kinetics of Iron Chelation and Release. In *Metal Ions in Biological Systems*; Sigel, A., Sigel, H., Eds.; Marcel Dekker: New York, 1998; pp 239−327.
(4) Raymond, K. N.; Dertz, E. A.; Kim, S. S. *Proc. Natl. Acad. Sci. U.S.A.* **2003**, *100*, 3584–3588.
(5) Dhungana, S.; Crumbliss, A. L. *Geomicrobiol. J.* **2005**, *22*, 87–98.
(6) Smith, M. J.; Ryan, D. E.; Nakanishi, K.; Frank, P.; Hodgson, K. O. Vanadium in Ascidians and the Chemistry of Tunichromes. In *Metal Ions in Biological Systems*; Marcel Dekker: New York, 1995; pp 423−430.
(7) Taylor, S. W.; Kammerer, B.; Bayer, E. *Chem. Rev.* **1997**, *97*, 333–346.
(8) Harris, W. R.; Carrano, C. J.; Cooper, S. R.; Sofen, S. R.; Avdeef, A. E.; McArdle, J. V.; Raymond, K. N. *J. Am. Chem. Soc.* **1979**, *101*, 6097–6104.
(9) Martell, A. E.; Smith, R. M. *Critical Stability Constants*; Plenum Press: New York, 1974−1977.
(10) Smith, M. J.; Kim, D.; Horenstein, B.; Nakanishi, K.; Kustin, K. *Acc. Chem. Res.* **1991**, *24*, 117–124.
(11) Sawada, H.; Yokosawa, H.; Lambert, C. C. *The Biology of Ascidians*; Springer: Tokyo, 2001.

Published on Web 10/12/2009

Chart 1

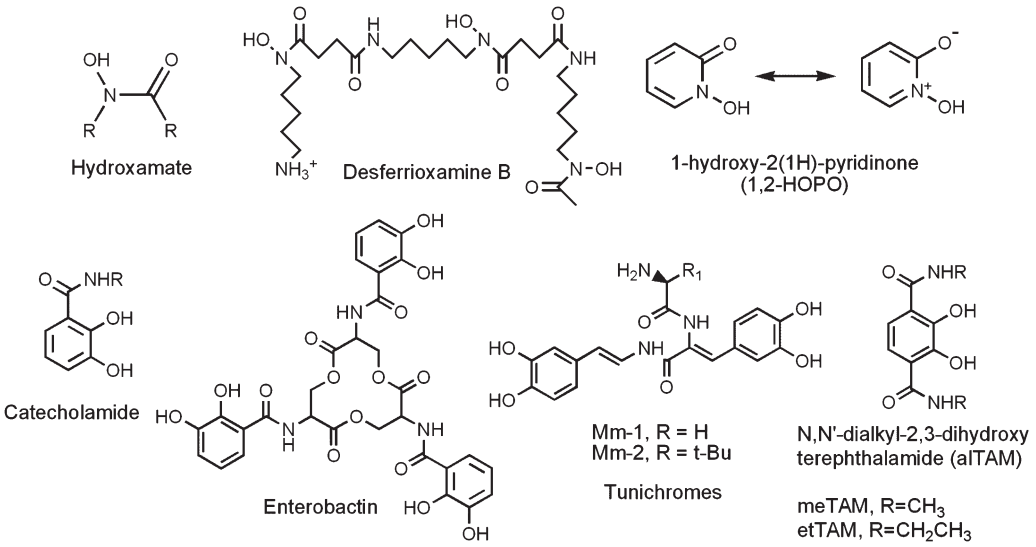

sequester extremely high levels of metals, including vanadium, iron, and even titanium, and tunichromes are often connected with this activity.[7,12] Although complexes of metals with tunichromes have been prepared in vitro, such complexes have not been observed in vivo or isolated from the organisms.[13−16] The function of tunichromes is still a matter of debate, with suggested alternative roles in metal reduction, wound repair, or tissue formation.[7] Some tunichromes have immunological properties, acting as antitumor, antibacterial, and antimicrobial agents.[17,18]

The strong chelating properties of catecholamides and hydroxamates inspired the development of simpler molecules that could be similarly beneficial in medicine, among other applications. One such set of catecholamide ligands is the *N*,*N*′-dialkyl-2,3-dihydroxyterephthalamide (alTAM) ligands. The alTAMs bind metals including Fe(III),[19,20] Th(IV),[21] Zr(IV),[21] Ce(IV),[21] and Ti(IV).[22] The hydroxypyridinones (HOPOs) are hydroxamate ligands used as models or substitutes for desferrioxamine B and related molecules. The HOPOs have been used in a variety of medicinal applications including in MRI contrast agents and in the removal of excess Fe from the body.[23] The X-ray crystal structures of the complexes of 1-hydroxy-2(1*H*)-pyridinone (1,2-HOPO) with Fe(III) are known with both 1:3 and 2:3 Fe/1,2-HOPO stoichiometry.[24,25] Their high stability constants[24,26] suggest these HOPOs as good candidates for metal chelation, which can be applied in medicine and can help model the solubilization of metals in nature.

In the present investigation, the complexes of Ti(IV) with the above ligands have been studied. Though titanium is not thought to be an essential element for human biology, there is evidence for its bioactivity, including in humans.[27−29] Some lower organisms sequester remarkable concentrations of Ti from the environment, the most avid of which is the ascidian *Eudistoma ritteri* (*E. ritteri*), which accumulates Ti in concentrations millions of times higher than that present in seawater.[30] Despite the ubiquity of titanium in biological systems and the environment, its biorelevant coordination chemistry remains incompletely explored.

Molecules similar to siderophores and tunichromes may promote the solubility of Ti(IV) and prevent its hydrolytic precipitation (ultimately as TiO_2) which is otherwise a serious impediment to its aqueous solubility. Catechol complexes of Ti have been known since 1920.[31] They were characterized, including by X-ray crystallography by Raymond et al.,[32] and their aqueous speciation[9,33,34] investigated. For hydroxamate ligands, there are fewer well-characterized Ti complexes. One features hydroxamate as well as tartrate and ethoxide ligands bound to a bridged titanium dimer.[35] A recently reported family of hydroxamate compounds

(12) Michael, J. P.; Pattenden, G. *Angew. Chem., Int. Ed. Engl.* **1993**, *32*, 1–23.
(13) Oltz, E. M.; Bruening, R. C.; Smith, M. J.; Kustin, K.; Nakanishi, K. *J. Am. Chem. Soc.* **1988**, *110*, 6162–6172.
(14) Oltz, E. M.; Pollack, S.; Delohery, T.; Smith, M. J.; Ojika, M.; Lee, S.; Kustin, K.; Nakanishi, K. *Experientia* **1989**, *45*, 186–190.
(15) Ryan, D. E.; Grant, K. B.; Nakanishi, K. *Biochemistry* **1996**, *35*, 8640–8650.
(16) Ryan, D. E.; Grant, K. B.; Nakanishi, K.; Frank, P.; Hodgson, K. O. *Biochemistry* **1996**, *35*, 8651–8661.
(17) Tincu, J. A.; Menzel, L. P.; Azimov, R.; Sands, J.; Hong, T.; Waring, A. J.; Taylor, S. W.; Lehrer, R. I. *J. Biol. Chem.* **2003**, *278*, 13546–13553.
(18) Rinehart, K. L. *Med. Res. Rev.* **2000**, *20*, 1–27.
(19) Garrett, T. M.; Miller, P. W.; Raymond, K. N. *Inorg. Chem.* **1989**, *28*, 128–133.
(20) Van Horn, J. D.; Gramer, C. J.; O′Sullivan, B.; Jurchen, K. M. C.; Doble, D. M. J.; Raymond, K. N. *C. R. Chim.* **2002**, *5*, 395–404.
(21) Gramer, C. J.; Raymond, K. N. *Inorg. Chem.* **2004**, *43*, 6397–6402.
(22) Davis, A. V.; Firman, T. K.; Hay, B. P.; Raymond, K. N. *J. Am. Chem. Soc.* **2006**, *128*, 9484–9496.
(23) Thompson, K. H.; Barta, C. A.; Orvig, C. *Chem. Soc. Rev.* **2006**, *35*, 545–556.
(24) Scarrow, R. C.; Riley, P. E.; Abudari, K.; White, D. L.; Raymond, K. N. *Inorg. Chem.* **1985**, *24*, 954–967.
(25) Scarrow, R. C.; White, D. L.; Raymond, K. N. *J. Am. Chem. Soc.* **1985**, *107*, 6540–6546.
(26) Li, Y. J.; Martell, A. E. *Inorg. Chim. Acta* **1993**, *214*, 103–111.
(27) Harding, M. M.; Mokdsi, G. *Curr. Med. Chem.* **2000**, *7*, 1289–1303.
(28) Melendez, E. *Crit. Rev. Oncol./Hematol.* **2002**, *42*, 309–315.
(29) Caruso, F.; Rossi, M. Antitumor Titanium Compounds and Related Metallocenes. In *Metal Ions in Biological Systems*; Sigel, A., Sigel, H., Eds.; Marcel Dekker: New York, 2004; pp 353−384.
(30) Levine, E. P. *Science* **1961**, *133*, 1352–1353.
(31) Rosenheim, A.; Sorge, O. *Chem. Ber.* **1920**, *53*, 932–939.
(32) Borgias, B. A.; Cooper, S. R.; Koh, Y. B.; Raymond, K. N. *Inorg. Chem.* **1984**, *23*, 1009–1016.
(33) Sommer, L. *Z. Anorg. Allg. Chem.* **1963**, *321*, 191–197.
(34) Sever, M. J.; Wilker, J. J. *Dalton Trans.* **2004**, 1061–1072.
(35) Williams, I. D.; Pedersen, S. F.; Sharpless, K. B.; Lippard, S. J. *J. Am. Chem. Soc.* **1984**, *106*, 6430–6431.

features 2,2′-bis(methylene)biphenyl-bridged bis(hydroxamate) or mixed hydroxamate/diketonate ligands.[36] Despite the lack of demonstrated aqueous stability for the foregoing two examples, there was some evidence that hydroxamate or related ligands might support the aqueous stability of Ti(IV).[37]

Taking inspiration from nature, ligands that are simple models of the siderophores and tunichromes were evaluated for their complexation properties toward Ti. Studies of the resulting complexes (Chart 2) will suggest whether these are likely ligands for Ti(IV) in biology and the environment, whether Ti(IV) might interfere with Fe(III) biogeochemical or in vivo nutrient cycling, and whether organisms might profitably use these ligands to control titanium trafficking. Given that the ligands have been proposed for applications like chelation therapy, avid binding to metals like Ti(IV) should be evaluated for its possible interference, and alternatively the Ti(IV) compounds may be medicinally valuable in their own right.

Experimental Section

General Procedures. All aqueous solutions were prepared with Nanopure-quality water (18.2 MΩ-cm resistivity; Barnstead model D11931 water purifier). 1-Hydroxy-2(1*H*)-pyridinone (1,2-HOPO) was purchased from Aldrich. KCl (J.T. Baker), which was used as the supporting electrolyte in the titrations, was used to prepare a 1.000 M stock solution in a volumetric flask. Elemental analysis was performed by Atlantic Microlabs (Norcross, Georgia).

Synthesis of alTAMs. The two ligands etTAM and meTAM were prepared following literature procedures.[19,38−40] The identity of each intermediate and product in the synthesis was verified by ^{1}H NMR spectroscopy.

Synthesis of $K_2[Ti(etTAM)_2(OCH_3)_2]\cdot 2CH_3OH$ (1). A 0.0132 M solution of etTAM was prepared in 3 mL of nitrogen-purged MeOH (Aldrich) by dissolving 0.01 g of etTAM (0.0396 mmol). In another round-bottom flask, 0.1 mL of $Ti(OEt)_4$ (67%, Alfa Aesar) was dissolved in 10 mL of MeOH in the presence of nitrogen. A 0.369 mL (0.0132 mmol) portion of the 0.0477 M $Ti(OEt)_4$ solution was added to the ligand solution and stirred for 2 h. The solution turned reddish-orange. A 0.159 mL portion of 0.5 M KOH (0.0795 mmol) in water was added, and the reaction mixture was stirred for 2 h. The solution was reduced to ∼0.5 mL by using a rotary evaporator. Yellow block X-ray quality crystals were observed after 2 weeks in the round-bottom flask. Yield: 0.0038 g (38.7%). Elemental analysis of $K_2TiC_{28}H_{42}N_4O_{12}$. Found (Calcd): C 44.46% (44.69%), H 5.38% (5.58%), N 7.61% (7.44%). UV/vis (H_2O): λ_{max} = 384 nm (ε_{384} = 8400 M^{-1} cm^{-1}). Mass spectrometry: $Na_2H[Ti(etTAM)_2(OCH_3)_2]^+$ (peaks ∼657 *m*/*z*) where the Na^+ are provided by the instrument and $K_3[Ti(etTAM)_3]^+$ (peaks ∼915 *m*/*z*).

In Situ Generation of $K_2[Ti(meTAM)_2(OCH_3)_2]$ (2). A similar procedure was followed for meTAM as above for etTAM. The amount of meTAM, $Ti(OEt)_4$, and KOH used were 0.01 g (0.0464 mmol), 0.432 mL of 0.0477 M solution (0.0149 mmol) in MeOH, and 0.186 mL of 0.5 M solution in water, respectively. UV/vis (H_2O): λ_{max} = 383 nm (ε_{383} = 5800 M^{-1} cm^{-1}). Mass spectrometry: $Na_2H[Ti(meTAM)_2(OCH_3)_2]^+$ (peaks ∼601 *m*/*z*) where the Na^+ are provided by the instrument and $K_3[Ti(meTAM)_3]^+$ (peaks ∼831 *m*/*z*).

Chart 2

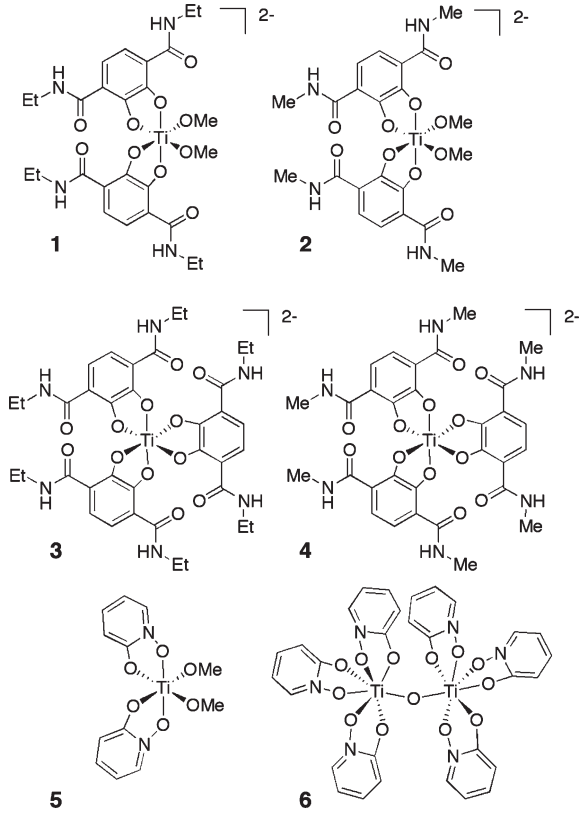

Preparation of $Na_2[Ti(etTAM)_3]$ (3). A 5 mL portion of *N*,*N*-dimethylformamide (DMF) was purged with nitrogen and 0.0156 g of $TiO(acac)_2$ (0.0595 mmol, Alfa Aesar) and 0.045 g of etTAM (0.1786 mmol) were added. The mixture was refluxed under N_2 for 12 h. The mixture was cooled to room temperature, 0.793 mL of 0.15 M $NaHCO_3$ solution (0.119 mmol) was added to it, and it was stirred for 2 h. The solvent was removed by rotary evaporator, and the solid was redissolved in MeOH. The mixture was filtered through Celite, and the solvent was removed from the filtrate to obtain a solid. Vapor-diffusion crystallizations with DMF as the solvent in the inner vial and EtOAc as the solvent in the outer vial yielded crystals. None were of sufficient quality for a complete structure refinement using X-ray crystallography because of structural disorder in the co-crystallized solvent. However, the connectivity between Ti and the ligands was clear. UV/vis (H_2O): λ_{max} = 400 nm (ε_{400} = 11010 M^{-1} cm^{-1}). Mass spectrometry: $Na_2H[Ti(etTAM)_3]^+$ (peaks ∼845.5 *m*/*z*).

In Situ Generation of $Na_2[Ti(meTAM)_3]$ (4). The general procedure above was followed as for (**3**). For the same weight of meTAM (0.045 g, 0.2009 mmol), the amount of $TiO(acac)_2$ added was 0.0175 g (0.06696 mmol), and the amount of 0.15 M $NaHCO_3$ solution added was 0.893 mL (0.1339 mmol). UV/vis (H_2O): λ_{max} = 394 nm (ε_{394} = 8600 M^{-1} cm^{-1}). Mass spectrometry: $Na_3[Ti(meTAM)_3]^+$ (peaks ∼783 *m*/*z*).

Preparation of $Ti(1,2\text{-}HOPO)_2(OCH_3)_2$ (5). A 5 mL portion of DMF was purged with nitrogen, and 0.02 g of 1,2-HOPO (0.18 mmol) and 0.01573 g of $TiO(acac)_2$ (0.06 mmol) were added to it. The mixture was refluxed overnight under nitrogen. The mixture was cooled, and 0.8 mL of 0.15 M $NaHCO_3$ solution (0.12 mmol) was added to it. The solvent was removed. The solid was redissolved in MeOH and filtered through Celite. The solvent was removed, and a brown solid obtained which was recrystallized from MeOH. Yield: 0.0065 g (32.8%). UV/vis

(36) Kongprakaiwoot, N.; Noll, B. C.; Brown, S. N. *Inorg. Chem.* **2008**, *47*, 11902–11909.
(37) Lobanov, F. I.; Savostina, V. M.; Fes′kova, V. M.; Shpigun, O. A.; Peshkova, V. M. *Russ. J. Inorg. Chem.* **1970**, *15*, 81–83.
(38) Dallacker, F.; Korb, W. *Liebigs Ann. Chem.* **1966**, *694*, 98–&.
(39) Weitl, F. L.; Raymond, K. N.; Durbin, P. W. *J. Med. Chem.* **1981**, *24*, 203–206.
(40) Gramer, C. J.; Raymond, K. N. *Org. Lett.* **2001**, *3*, 2827–2830.

(MeOH): $\lambda_{max} = 309$ nm ($\varepsilon_{309} = 2450\ M^{-1}\ cm^{-1}$), UV/vis ($H_2O$): $\lambda_{max} = 304$ nm ($\varepsilon_{304} = 5330\ M^{-1}\ cm^{-1}$). Mass spectrometry in water: $Na[Ti(1,2\text{-}HOPO)_2(OCH_3)_2]^+$ (peaks ~353 m/z), $[Ti(1,2\text{-}HOPO)_3]^+$ (peaks ~378 m/z) and $[Ti_2(1,2\text{-}HOPO)_4(OCH_3)(OH)(acac)]^+$ (peaks ~683 m/z). Mass spectrometry in MeOH: $Na[Ti(1,2\text{-}HOPO)_2(OCH_3)_2]^+$ (peaks ~353 m/z), and $[Ti_2(1,2\text{-}HOPO)_4(OCH_3)(OH)(acac)]^+$ (peaks ~683 m/z).

Preparation of [(1,2-HOPO)$_3$TiOTi(1,2-HOPO)$_3$] (6). A flask was purged with nitrogen, and 0.030 g of $TiCl_3$ (0.20 mmol) added to it. In a second flask, 0.067 g of 1,2-HOPO (0.60 mmol) in 10 mL of water was purged with nitrogen. The 1,2-HOPO solution was transferred to the $TiCl_3$ by syringe while both were under nitrogen, and the solution was stirred under nitrogen for 90 min. The solution was bubbled with air for 90 min as the Ti(III) solution oxidized to a yellow Ti(IV) solution. The pH was determined to be 1.75. The bright yellow solid product was collected by filtration. Yellow crystals of $[(1,2\text{-}HOPO)_3TiOTi(1,2\text{-}HOPO)_3]$ (**6**) grew from the filtrate upon standing. Multiple attempts yielded unsatisfactory elemental analyses of the bulk yellow solid; the solid is probably a mixture, matching most closely with $(1,2\text{-}HOPO)_2Ti(OH)_2$ Found (Calcd for $TiC_{10}H_{10}O_6N_2$): C 39.86% (39.76%), H 3.90% (3.33%), N 8.62% (9.27%).

Preparation of Solutions for the Titrations. Carbonate-free KOH was prepared from a (1.0 M) stock solution (Dilut-It Concentrate, J. T. Baker) and was standardized against potassium hydrogen phthalate (Mallinckrodt) by using phenolphthalein (1% in 95% alcohol, Mallinckrodt) as an indicator. A Gran's plot analysis was performed to confirm the absence of carbonate (data not shown). Similarly, HCl solutions (J. T. Baker) were standardized against KOH using phenolphthalein as indicator.

Spectropotentiometric Titrations. The titration apparatus consisted of a 100 mL water jacketed vessel (Kontes Co.) attached to a thermostatted water bath.[41−43] The temperature was maintained at 25 °C during the titration. The lid of the vessel had four holes: one each for the pH combination electrode, UV/vis probe, base additions and argon gas. The holes were fitted with appropriate connectors, stoppers, and rubber septa, and the lid was sealed to the glass titration vessel with the help of a silicon rubber seal (McMaster Carr Co.). A positive flow of argon gas was maintained in the vessel throughout all the titrations.

The pH was monitored as mV readings by using an Orion model 520 pH meter (accurate to 0.1 mV) and an Orion pH electrode (model 8102BNU). The electrode was calibrated before each titration by measuring the voltage after the addition of known volumes of KOH to a 50 mL HCl solution containing 0.1 M KCl at 25 °C. Resulting Nernst equations were used to convert mV readings to pH.

A stock solution (0.0881 M) of the etTAM ligand was prepared in MeOH (HPLC grade, Aldrich). A $TiCl_4$ stock solution was prepared in water by the addition of 20 μL of $TiCl_4$ (99.9%, Aldrich) to 10 mL of ice-cooled water, purged with nitrogen. The titanium concentration was confirmed by using a Varian SpectrAA-20 flame atomic absorption spectrometer. The standards used to calibrate the instrument were prepared from a 1000 ppm Ti atomic absorption standard in acid (Rikka Chemical Co.). Samples were analyzed in triplicate. The Ti concentration was further confirmed by a colorimetric assay by using 2,3-dihydroxynaphthalene-6-sulfonic acid (TCI America) as the chelator.[44]

For the titration of the etTAM ligand alone in water, the titration solution was prepared with a final volume of 50 mL containing 3.524×10^{-4} M etTAM in MeOH and 0.1 M KCl as the supporting electrolyte. The final amount of MeOH in the solution was only 0.4%. The pH was increased by using 0.09893 M KOH to ~11 before the volume was adjusted to 50 mL with water by using a volumetric pipet. When the titration was attempted from low pH, precipitation was observed at pH 2.7. Once the precipitation takes place, it is difficult for the neutral ligand to dissolve because of the low MeOH concentration of the solution. However, the titration was reversible when started from a high pH to a pH of 3. Equilibrium was achieved when the mV reading was constant for at least 2 min, and the corresponding reading was noted. In addition to the potentiometric data, UV/vis absorbance data were collected on a Varian Cary 50 UV/vis spectrometer between 200 and 600 nm. The data were collected by using a 0.2 cm path length dip probe and coupler (Varian parts 79−100326 and 02−101593, respectively).

For the titration of Ti and etTAM systems, the concentration of the Ti was varied in the solutions keeping the concentration of etTAM constant such that different Ti/etTAM ratios were achieved including 1:2, 1:3, and 1:4. The titration solution was prepared with a final volume of 50 mL containing 3.524×10^{-4} M etTAM, 0.1 M KCl as the supporting electrolyte, added $TiCl_4$ such that the specified mole ratio is achieved and ~2−2.4 mL of 0.09893 M KOH such that the starting pH is ~10. The ligand was added as a solution in MeOH (0.4% final concentration MeOH). The solution was titrated with acid similar to the ligand-only titration. The millivolt readings and UV/vis scans were collected after addition of each aliquot and equilibration. In the region near the inflection point, the equilibration took more than several hours to attain and hence some titrations took overall more than 30 h. About 50−70 data points were collected for each titration, in a pH range of 2.8−10. The metal−ligand titrations were reversible in this pH range. As for the ligand alone, below pH 2.8, precipitation was observed in the solution.

Least Squares Fitting. The pH dependent UV/vis absorbance data were used to model the speciation in solution at different pH values by using the programs Specfit/32[45−49] and HypSpec.[50] Using first the model-free factor analysis, significant factors corresponding to the different colored species were estimated independent of any model and their contributions as a function of pH evaluated. The species corresponding to the factors were then fitted when postulating a wide variety of proposed ternary metal−ligand-proton species, and the log beta values for each species refined.

Physical Measurements. The electrospray mass spectra of the aqueous solutions of the Ti complexes were collected on Waters/Micromass ZQ spectrometer at a capillary voltage of 3 kV, cone voltage of ~30 V, and extractor voltage of 3 V. ^{1}H NMR spectra were recorded on a Bruker Avance 400 MHz spectrometer either in DMSO or in $CHCl_3$ depending on the solubility of each intermediate and product.

Cyclic Voltammetry. The cyclic voltammograms were recorded on a Metroohm 746 VA trace analyzer and a 747 VA stand. The Ag/AgCl/3 M KCl electrode was used as the reference electrode, the hanging mercury drop electrode as the

(41) Martell, A. E.; Motekaitis, R. J. *Determination and Use of Stability Constants*; Wiley-VCH: New York, 1992.
(42) Martell, A. E.; Hancock, R. D. *Metal Complexes in Aqueous Solutions*; Plenum Press: New York, 1996.
(43) Collins, J. M.; Uppal, R.; Incarvito, C. D.; Valentine, A. M. *Inorg. Chem.* **2005**, *44*, 3431–3440.
(44) Tinoco, A. D.; Incarvito, C. D.; Valentine, A. M. *J. Am. Chem. Soc.* **2007**, *129*, 3444–3454.
(45) Binstead, R. A.; Jung, B.; Zuberbuhler, A. D. *Specfit/32*; Software Associates: Marlborough, MA, 2001.
(46) Gampp, H.; Maeder, M.; Meyer, C. J.; Zuberbuhler, A. D. *Talanta* **1985**, *32*, 95–101.
(47) Gampp, H.; Maeder, M.; Meyer, C. J.; Zuberbuhler, A. D. *Talanta* **1985**, *32*, 257–264.
(48) Gampp, H.; Maeder, M.; Meyer, C. J.; Zuberbuhler, A. D. *Talanta* **1985**, *32*, 1133–1139.
(49) Gampp, H.; Maeder, M.; Meyer, C. J.; Zuberbuhler, A. D. *Talanta* **1986**, *33*, 943–951.
(50) Gans, P.; Sabatini, A.; Vacca, A. *Talanta* **1996**, *43*, 1739–1753.

working electrode, and a platinum wire as the auxiliary electrode. Potentials are reported versus NHE. A 0.1 M KNO_3 (Fisher, ACS-grade) solution was used as a supporting electrolyte. A blank profile was acquired with a 0.1 M KNO_3 solution in 20% MeCN/80% H_2O. A 4 mM solution of etTAM and complex **1** was prepared in 20% MeCN/80% H_2O, containing 0.1 M KNO_3 and scanned at the rate of 100 mV/s in the scan range of −0.7 V to −1.6 V.

X-ray Structure Determination for the Complexes. Crystals were mounted with epoxy cement on the tips of fine glass fibers. The data were collected on a Nonius KappaCCD diffractometer with graphite monochromatic Mo Kα radiation. The data frames were scaled and processed by using the DENZO software package.[51] The data were corrected for Lorentz and polarization effects and no absorption correction was applied. The structures were solved by direct methods and expanded by using Fourier techniques. The non-hydrogen atoms were refined anisotropically and hydrogen atoms were treated as idealized contributions. For complex **1**, a yellow block crystal having dimensions of 0.10 × 0.10 × 0.10 mm^3 was mounted. A total of 15490 reflections were collected of which 8642 were unique and observed (R_{int} = 0.1240). The data were acquired at 173(2) K to a maximum 2θ value of 56.56°. The hydrogen atoms on the amide N and those on the MeOH molecules in complex **1** were located from the residual electron difference map and refined with isotropic displacement parameters. For complex **5**, a pale yellow block crystal having dimensions of 0.20 × 0.10 × 0.10 mm^3 was mounted. A total of 5630 reflections were collected of which 3513 were unique and detected (R_{int} = 0.0317). The data were collected at 123(2) K to a maximum 2θ value of 58.98°. For complex **6**, a colorless block crystal having approximate dimensions of 0.20 × 0.10 × 0.10 mm^3 was mounted. The data were collected at 173(2) K to a maximum 2θ value of 57.56°. A total of 15030 reflections were collected of which 9159 were unique and observed (R_{int} = 0.0928). The hydrogen atoms of the co-crystallized waters in complex **6** could not be located. Relevant crystallographic data appear in Table 1.

Table 1. Crystallographic Data for $K_2[Ti(etTAM)_2(OCH_3)_2]\cdot 2CH_3OH$ (**1**), $[Ti(1,2\text{-}HOPO)_2(OCH_3)_2]$ (**5**), and $[(1,2\text{-}HOPO)_3TiOTi(1,2\text{-}HOPO)_3]$ (**6**)

compound number	**1**	**5**	**6**
chemical formula	$C_{28}H_{42}K_2N_4O_{12}Ti$	$C_{12}H_{14}N_2O_6Ti$	$C_{30}H_{24}N_6O_{19}Ti_2$
formula weight	752.76	330.15	862.43
a (Å)	9.6651(19)	9.5453(19)	10.954(2)
b (Å)	16.754(3)	11.149(2)	12.906(3)
c (Å)	21.680(4)	13.218(3)	13.140(3)
α (deg)	90	90	81.88(3)
β (deg)	94.55(3)	97.02(3)	86.79(3)
γ (deg)	90	90	75.70(3)
V (Å^3)	3499.5(12)	1396.1(5)	1781.6(6)
Z	4	4	2
space group	$P2_1/c$	$P2_1/n$	$P\bar{1}$
T (K)	173(2)	123(2)	173(2)
λ	Mo Kα, 0.71073 Å	Mo Kα, 0.71073 Å	Mo Kα, 0.71073 Å
D_{calcd} (g cm^{-3})	1.429	1.571	1.608
μ (cm^{-1})	5.46	6.42	5.38
R^a	0.0649[b]	0.0433[c]	0.0916[d]
$R_w{}^a$	0.0945[b]	0.1136[c]	0.1850[d]

[a] R values are based on F; R_w values are based on F^2, $R = \sum||F_o| - |F_c||/\sum|F_o|$, $R_w = (\sum w(F_o{}^2 - F_c{}^2)^2/\sum w(F_o{}^2)^2)^{1/2}$. [b] For 8642 reflections with $I > 2\sigma(I)$. [c] For 3513 reflections with $I > 2\sigma(I)$. [d] For 9159 reflections with $I > 2\sigma(I)$.

Results

Characterization of the Ti Complexes of etTAM. Synthesis. The Ti complexes of etTAM were synthesized by two different methods using different sources of Ti. For the 1:2 Ti/etTAM complex **1**, $Ti(OEt)_4$ was used as the starting material, and the pH after dissolution of the crystals was ∼8.7. Potential alkoxide ligands were avoided during the synthesis of the 1:3 Ti/etTAM complex **3**. Instead, $TiO(acac)_2$ was used as the starting material, methanol was removed by rotary evaporation, and the compound was crystallized in its absence. Because a non-aqueous solvent was used for the synthesis, the pH of the reaction mixture could not be measured. However, the dissolution of the crystals in water gave a solution with a pH of 7.5.

Description of the X-ray Crystal Structure of Complex 1. Complex **1** crystallizes in a monoclinic space group $P2_1/c$ with one titanium complex in the asymmetric unit and four in each unit cell. The geometry around each Ti can be best described as a distorted octahedral geometry with each of the bidentate etTAM ligands binding symmetrically with respect to the Ti−O bonds. The coordination sphere is completed by two anionic methoxide ligands. The X-ray crystal structure of the complex is given in Figure 1. Relevant crystallographic parameters are given in Table 1, and selected bond distances and bond angles are presented in Table 2. Two potassium ions are bound by the dianionic complex to balance the charge, and two molecules of methanol are present as molecules of solvation.

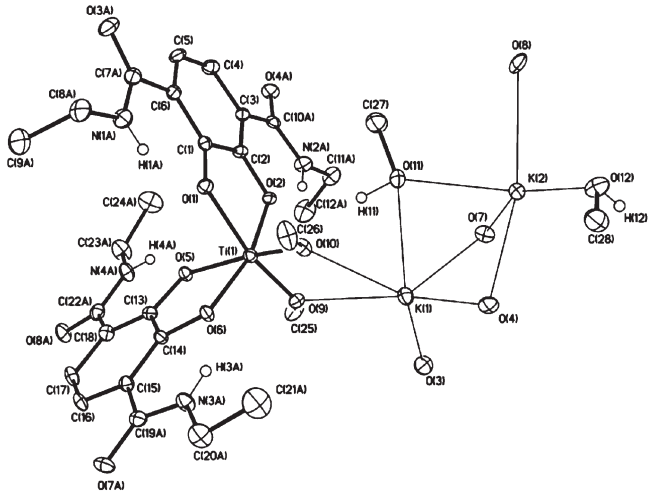

Figure 1. ORTEP diagram of $K_2[Ti(etTAM)_2(OCH_3)_2]\cdot 2CH_3OH$, complex **1**.

An extended structure is formed by potassium−oxygen interactions involving both the titanium complex and the free methanol molecules. Linear tetramers of potassium atoms, exhibiting two different potassium environments, are the core repeating component of the extended structure as is illustrated in Supporting Information, Figure S1. K(1) is bound to six oxygen atoms, two from the μ-OCH_3 ligands bridging K(1) and Ti(1), three donated by the bidentate ligands, and the final oxygen donated by the μ-$HOCH_3$ solvent molecule bridging K(1) and K(2). A different type of coordination is observed for K(2), in which it is bound to seven oxygen atoms. Two of the oxygen atoms are donated by bidentate etTAM molecules

(51) Otwinowski, Z.; Minor, W. Processing of X-ray diffraction data collected in oscillation mode. In *Macromolecular Crystallography, Pt A*; Carter, C. W., Jr., Sweet, R. M., Eds.; Academic Press: San Diego, **1997**; Vol. *276*, pp 307−326.

Table 2. Selected Bond Lengths (Å) and Angles (deg) for the Complex **1**

Ti(1)−O(9)	1.8429(16)	O(9)−Ti(1)−O(5)	92.39(7)
Ti(1)−O(10)	1.8765(16)	O(10)−Ti(1)−O(5)	164.83(7)
Ti(1)−O(2)	1.9890(17)	O(2)−Ti(1)−O(5)	86.92(6)
Ti(1)−O(6)	1.9905(17)	O(6)−Ti(1)−O(5)	77.87(7)
Ti(1)−O(5)	2.0118(16)	O(9)−Ti(1)−O(1)	162.50(7)
Ti(1)−O(1)	2.0182(16)	O(2)−Ti(1)−O(1)	90.35(7)
	2.0182(16)	O(2)−Ti(1)−O(1)	77.42(6)
Ti(1)−K(1)	3.8149(13)	O(6)−Ti(1)−O(1)	94.74(7)
		O(5)−Ti(1)−O(1)	87.23(6)
O(9)−Ti(1)−O(10)	94.37(7)	O(9)−Ti(1)−K(1)	41.45(5)
O(9)−Ti(1)−O(2)	85.09(7)	O(10)−Ti(1)−K(1)	54.95(5)
O(10)−Ti(1)−O(2)	107.17(7)	O(2)−Ti(1)−K(1)	86.28(5)
O(9)−Ti(1)−O(6)	102.29(7)	O(6)−Ti(1)−K(1)	109.26(5)
O(10)−Ti(1)−O(6)	87.41(7)	O(5)−Ti(1)−K(1)	133.75(5)
O(2)−Ti(1)−O(6)	163.27(6)	O(1)−Ti(1)−K(1)	135.14(5)

and the third by the μ-$HOCH_3$ solvent molecule bridging K(1) and K(2). The other four oxygen atoms come from two other bridging bidentate ligands and two μ-$HOCH_3$ solvent molecules bridging K(2) and K(3). In addition to the extended network formed by the potassium ions and solvent molecules, intramolecular interactions were also observed between the N−H and catecholic O atoms of the ligands as illustrated in Supporting Information, Figure S2. The interatomic distances between the N−H hydrogen and the catecholic O are 1.99 and 1.97 Å for H(1)···O(1) and H(2)···O(2), respectively.

Description of the Structure of Complex 3. Complex **3** was crystallized by diffusion of EtOAc into the sample dissolved in DMF. A few DMF molecules co-crystallized along with two Na^+ counter cations. The identity and connectivity of the complex are unambiguous from the crystallographic data obtained. However, the resolution and particularly the disorder of the co-crystallized solvent led to unstable further refinement. The geometry around the Ti is distorted octahedral with three bidentate ligands binding the metal atom. The structure is shown in Figure 2 and more details appear in Supporting Information, Figure S3.

Electrospray Mass Spectrometry for the Ti(IV) Complexes of etTAM. The electrospray mass spectrum of complex **1** dissolved in water confirms the presence of both the 1:2 and 1:3 species in solution. The peaks at a m/z of ~657 are consistent with $Na_2H[Ti(etTAM)_2(OCH_3)_2]^+$. The peaks at a m/z ~915 are consistent with $K_3[Ti(etTAM)_3]^+$, a 1:3 Ti/etTAM complex. Figure 3 shows the titanium isotope distributions overlaid on the experimental spectrum.

The mass spectrum of complex **3** dissolved in water (Supporting Information, Figure S4) at pH 7.5 shows the presence of a 1:3 species in solution with several other fragments from the 1:3 species. Although it is predicted to occur at this pH (see below), a 1:2 metal/ligand species was not detected in the mass spectrum. It could be that this anionic complex is insufficiently basic to be protonated and/or does not have sufficient affinity for alkali metal cations to be visible in the positive ion mass spectrometer.

Cyclic Voltammetry for Complex 1. Cyclic voltammetry was performed on etTAM ligand alone in a 0.1 M KNO_3 solution in 20% MeCN/80% H_2O with the hanging mercury drop electrode as the working electrode. MeCN was required as a cosolvent because the ligand is not soluble in water. The profile was similar to the blank

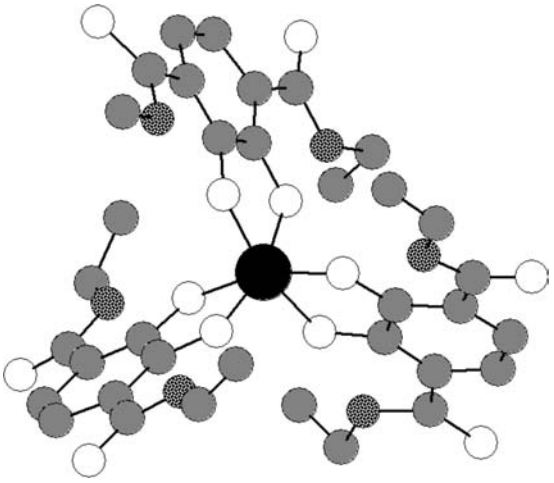

Figure 2. Structure of the $[Ti(etTAM)_3]^{2-}$ anion of $Na_2[Ti(etTAM)_3]$, complex **3**, showing the connectivity of the ligands to the metal. Spheres in the structure represent: black, titanium; white, oxygen; gray, carbon; dotted, nitrogen. Hydrogen atoms are not shown in the figure.

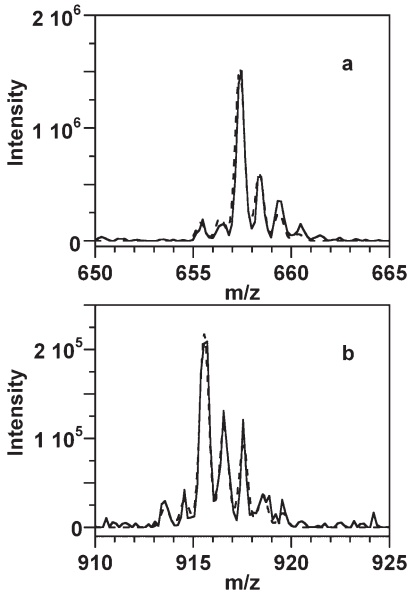

Figure 3. ESI-MS of complex **1** in water showing peaks consistent with titanium isotope distributions for (a) $Na_2H[Ti(etTAM)_2(OCH_3)_2]^+$ (peaks ~657 m/z) where the Na^+ are provided by the instrument and (b) $K_3[Ti(etTAM)_3]^+$ (peaks ~915 m/z). Experimental spectrum, solid line; simulated titanium isotope distributions, dashed line.

profile obtained for the supporting electrolyte solution (0.1 M KNO_3) with no peaks observed (data not shown). Even though the complex is soluble in water, the solution of complex **1** was prepared in the same MeCN/H_2O mixture containing the supporting electrolyte to keep all the conditions the same. The cyclic voltammogram of the solution of complex **1** (Supporting Information, Figure S5) showed a reversible wave with an $E_{1/2}$ of −0.98 V. The difference between the E_{ox} and E_{red} is ~63 mV.

Spectropotentiometric Titrations of Ti/etTAM Complexes. Because the ligand is insoluble in water, it was dissolved in a small amount of MeOH. The final methanol concentration for the titrations after dilution was just 0.4%. The initial pH for each titration was ~10 and decreased by the addition of acid. The millivolt readings

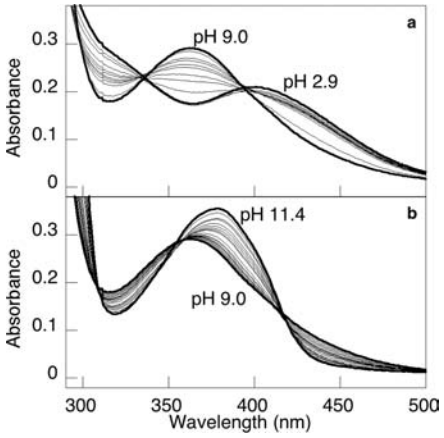

Figure 4. Selected spectra from the spectropotentiometric titration of a 1:3 Ti/etTAM solution shown for reference. **a.** Selected spectra between pH 2.9 and pH 9.0. **b.** Selected spectra between pH 9.0 and pH 11.4.

were noted, and the UV/vis spectra scanned after equilibration. The data were fit with Specfit/32 and HypSpec and the pK_a values for the two catechol protons were determined. The formation constants measured were log β_{011} = 10.98 and log β_{012} = 17.26, in good agreement with the literature values.[19,20] The stability constants and spectra for the three ligand species were fixed in the analysis of the subsequent titrations with titanium.

Metal/ligand titrations were performed with varied ratios of metal/ligand including 1:2, 1:3, and 1:4. The data for all the titrations were reversible between pH range 3−10. Precipitation was observed below pH 3 and thus those data were not used for fitting. Some representative data for a 1:3 Ti/etTAM titration are shown in Figure 4.

From the model-free analysis, it was evident that six colored species were required to account for all the absorbance changes, and these six species include the three colored forms of the free ligand. Thus, three metal-containing species are required to fit the data. The species that predominates at the lowest pH, having λ_{max} = 400 nm and $\varepsilon_{400\ nm}$ = 8300 M^{-1} cm^{-1}, is well modeled as a $Ti(etTAM)_3^{2-}$, or a MLH 130 species. Its optical spectrum agrees well with that reported for the tris-catechol species (λ_{max} = 389 nm and ε = 9300 M^{-1} cm^{-1}),[32] including an intense absorption below 300 nm, and with the anion of **3** (λ_{max} = 400 nm and ε = 11010 M^{-1} cm^{-1}). Because this species is formed to its fullest extent even at pH 3 and there is no observable Ti^{4+}(aq) (or hydrolyzed species thereof) even at this very low pH, a proper β_{130} stability constant cannot be obtained from these data; however, to overcome the powerful titanium hydrolysis at this pH,[52−54] our models suggest that log β_{130} must be ≥55. This value is consistent with the one for Ti binding to catechol (log β_{130} = 60.3).[32,55]

The signal for this species begins to decrease in concentration at pH 6, and a more-hydrolyzed species, the spectrum of which also was evident at lower pH values, increases in concentration. The latter is best modeled at the hydrolysis level of MLH 12−2. This species features 1 metal ion, 2 deprotonated ligands, and formally −2 protons. The "negative protons" will come from water, so the species could be formulated as $Ti(etTAM)_2(OH)_2^{2-}$ or $TiO(etTAM)_2^{2-}$. The spectropotentiometry would not distinguish between the bis-hydroxo and the mono-oxo species, because they are both at the same hydrolysis level. Alternatively, dimerization of these species (with loss of water for the former) would afford the $[(cat)_2TiO]_2^{4-}$ species observed with catechol.[32] The UV/vis spectrum of the current species (λ_{max} = 360 nm and ε = 9500 M^{-1} cm^{-1} per Ti) matches well with the solid state UV/vis spectrum for $[(cat)_2TiO]_2^{4-}$ and with the solution spectrum of complex **1** in solution (λ_{max} = 384 nm and ε = 8400 M^{-1} cm^{-1}).

Above pH 9, this second species decreases because of further hydrolysis, though no precipitation is observed. The UV/vis spectrum of the fully protonated ligand accounts for most of the spectral intensity observed at the highest pH values, suggesting that the high-pH metal-containing species has few if any ligands bound and/or little or no absorbance in the region probed. This high pH species could be modeled well as a $Ti(etTAM)(OH)_4^{2-}$ (MLH 11−4) species, with a UV/vis spectrum somewhat similar to that of the deprotonated ligand $etTAM^{2-}$. Alternatively, if a soluble but UV/vis silent five-time hydrolyzed $Ti(OH)_5^-$ species was included in the model, as some aqueous speciation data support,[54] though other data do not,[53] then the highest pH species could be modeled as this moiety. Other species, including $Ti(etTAM)^{2+}$ (MLH 110), $Ti(etTAM)_2$ (MLH 120), $Ti(etTAM)_3OH^{3-}$ (MLH 13−1) or its dimer, or $Ti(etTAM)_2(O)(OH)^{3-}$ (MLH 12−3), were not supported by the data.

$$Ti^{4+} + 3etTAM^{2-} \leftrightarrows Ti(etTAM)_3^{2-} \qquad \beta_{130} \quad (1)$$

$$Ti^{4+} + 2etTAM^{2-} + 2H_2O \leftrightarrows Ti(etTAM)_2(OH)_2^{2-} + 2H^+ \qquad \beta_{12-2} \quad (2)$$

$$Ti^{4+} + etTAM^{2-} + 4H_2O \leftrightarrows Ti(etTAM)_2(OH)_4^{2-} + 4H^+ \qquad \beta_{11-4} \quad (3)$$

The data were best modeled by MLH 130, MLH 12−2, and MLH 11−4 species having log β_{MLH} values of 59.5, 37.5, and 12.2, respectively (Figure 5). These values should not be taken as rigorously determined stability constants, because as described above the β_{130} value cannot be accurately determined when the complex does not dissociate to Ti^{4+} ions at the lowest pH values. A log β_{130} less than 55 returns a model having less than full complex formation at pH 3, which is inconsistent with the data. But each log β above might be larger by the same factor, and the data would not reveal this fact. However, the pH-dependent speciation in Figure 5 and the relative log K values are revealed; for example, the equilibrium

(52) Ciavatta, L.; Ferri, D.; Riccio, G. *Polyhedron* **1985**, *4*, 15–21.
(53) Sugimoto, T.; Zhou, X. P.; Muramatsu, A. *J. Colloid Interface Sci.* **2002**, *252*, 339–346.
(54) Knauss, K. G.; Dibley, M. J.; Bourcier, W. L.; Shaw, H. F. *App. Geochem.* **2001**, *16*, 1115–1128.
(55) Sommer, L. *Collect. Czech. Chem. Commun.* **1963**, *28*, 2102 ff.

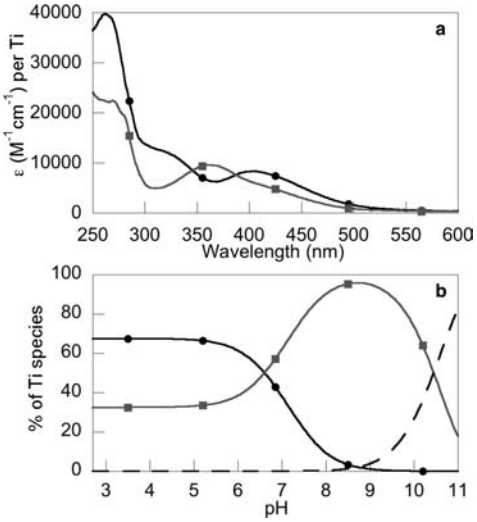

Figure 5. Speciation of Ti(IV) and etTAM. **a.** Spectra of the two metal containing species that predominate between pH 3 and pH 10, MLH 130 ($[Ti(etTAM)_3]^{2-}$) (●) and MLH 12−2 ($[Ti(etTAM)_2(OH)_2]^{2-}$ or its equivalent) (■). **b.** Concentration of these species as a function of pH at a 1:3 metal/ligand ratio. Above pH 9, the $[Ti(etTAM)_2(OH)_2]^{2-}$ level hydrolysis species converts to a more hydrolyzed species (see text).

constant for conversion of the MLH 130 to the MLH 120 species (eq 4) is log $K = -22$.

$$Ti(etTAM)_3^{2-} + 2H_2O \leftrightarrows Ti(etTAM)_2(OH)_2^{2-} + etTAM^{2-} + 2H^+ \quad (4)$$

The same model accounted for the spectral data for two independent 1:3 metal/ligand titrations as well as replicate titrations at 1:2 and 1:4 metal/ligand ratios.

Characterization of the Ti Complexes of meTAM. The complexes **2** and **4** were synthesized as given above in the Experimental Section and were characterized in solution by mass spectrometry. The mass spectrum of complex **2** in water showed the presence of the 1:2 and the 1:3 species as observed in the case of etTAM. The peaks ~601 and ~831 m/z are consistent with titanium isotope distributions for $Na_2H[Ti(meTAM)_2(OCH_3)_2]^+$ and $K_3[Ti(meTAM)_3]^+$, respectively (Supporting Information, Figure S6).

The mass spectrum of complex **4** in water displayed only the 1:3 species in solution; no 1:2 species was observed (Supporting Information, Figure S7).

Synthesis of Ti Complexes of 1,2-HOPO. Description of the X-ray Crystal Structure of Complex 5. Complex **5** crystallizes in a monoclinic space group $P2_1/n$ with one titanium complex in the asymmetric unit and four in each unit cell. The complex crystallizes with a distorted octahedral geometry around the Ti atom. The two bidentate 1,2-HOPO ligands bind symmetrically around the Ti atom, and the coordination sphere is completed by two anionic methoxide ligands. The X-ray crystal structure of the complex is given in Figure 6. Relevant crystallographic parameters are given in Table 1, and selected bond distances and bond angles are presented in Table 3. Because the two 1,2-HOPO ligands are monoanionic, the complex is neutral. The complex does not crystallize with any solvent molecules. The molecule possesses a pseudo-2-fold axis of rotation as illustrated in Supporting Information, Figure S8. The complex also displays π-stacking

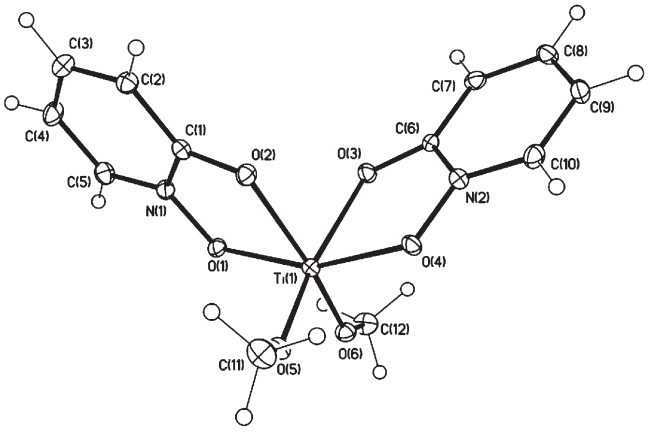

Figure 6. ORTEP diagram of $[Ti(1,2\text{-}HOPO)_2(OCH_3)_2]$, complex **5**.

Table 3. Selected Bond Lengths (Å) and Angles (deg) for the Complex **5**

Ti(1)−O(6)	1.8429(16)	O(6)−Ti(1)−O(2)	162.79(6)
Ti(1)−O(5)	1.8765(16)	O(5)−Ti(1)−O(2)	91.58(6)
Ti(1)−O(4)	1.9890(17)	O(4)−Ti(1)−O(2)	88.45(6)
Ti(1)−O(1)	1.9905(17)	O(1)−Ti(1)−O(2)	76.62(6)
Ti(1)−O(2)	2.0118(16)	O(6)−Ti(1)−O(3)	90.19(7)
Ti(1)−O(3)	2.0182(16)	O(5)−Ti(1)−O(3)	162.43(6)
		O(4)−Ti(1)−O(3)	76.29(6)
O(6)−Ti(1)−O(5)	98.47(7)	O(1)−Ti(1)−O(3)	89.02(6)
O(6)−Ti(1)−O(1)	87.10(6)	O(2)−Ti(1)−O(3)	84.08(6)
O(5)−Ti(1)−O(1)	106.57(7)	O(5)−Ti(1)−O(4)	86.60(6)
O(4)−Ti(1)−O(1)	160.13(6)	O(6)−Ti(1)−O(4)	105.97(7)

between the phenyl rings of different molecules (Supporting Information, Figure S9). Another interesting feature in the structure is the trans orientation of the NO-Ti bonds of the two 1,2-HOPO ligands.

Mass Spectrometry of Complex 5. The mass spectrum of complex **5** in water displayed several species. The peaks ~353 m/z and ~378 m/z correspond to titanium isotope distributions of $Na[Ti(1,2\text{-}HOPO)_2(OCH_3)_2]^+$ and $[Ti(1,2\text{-}HOPO)_3]^+$ (Supporting Information, Figure S10). The former is similar to the X-ray crystal structure of **5**. A dimeric species $[Ti_2(1,2\text{-}HOPO)_4(OCH_3)(OH)(acac)]^+$ was also present in significant quantities in the solution and was observed in the spectrum at 683 m/z.

The mass spectrum of complex **5** in MeOH exhibited peaks with titanium isotope distributions consistent with the monomeric species $Na[Ti(1,2\text{-}HOPO)_2(OCH_3)_2]^+$ and the dimeric species $[Ti_2(1,2\text{-}HOPO)_4(OCH_3)(OH)(acac)]^+$ in solution. No 1:3 Ti/1,2-HOPO species was observed in the spectrum.

Description of the X-ray Crystal Structure of Complex 6. When the 1,2-HOPO complex of Ti(IV) was prepared in the absence of potential alkoxide ligands, elemental analysis of the bulk solid that formed suggested a 2:1 1,2-HOPO/Ti complex, consistent with the results above. However, the species that crystallized was a neutral dimer having 7-coordinate titanium(IV) ions with three bidentate 1,2-HOPO ligands on each metal as well as a nearly linear (158°) oxo bridge (Figure 7). Selected bond lengths and angles are given in Table 4. The geometry at each titanium is nearly pentagonal bipyramidal, with the oxo bridge and one ligand oxygen at the axial positions, and the remainder of the ligand oxygens nearly in a plane slightly distorted away from the oxo bridge. The data were best modeled by having a NO oxygen donor at the axial position on one side of the molecule and a carbonyl

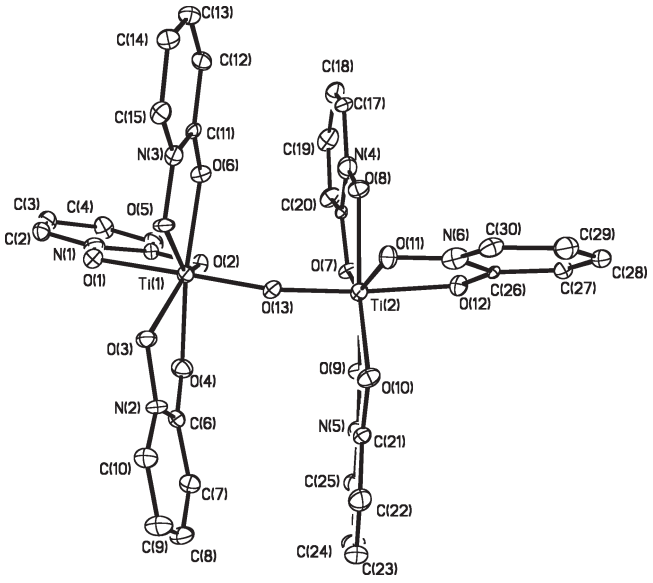

Figure 7. ORTEP diagram of $[(1,2\text{-HOPO})_3\text{TiOTi}(1,2\text{-HOPO})_3]$, complex **6**.

Table 4. Selected Bond Lengths (Å) and Angles (deg) for Complex **6**

Ti(1)−O(1)	2.062(3)	Ti(1)−O(13)−Ti(2)	158.0(2)
Ti(1)−O(2)	2.050(4)	O(13)−Ti(1)−O(1)	168.75(15)
Ti(1)−O(3)	2.030(3)	O(13)−Ti(1)−O(2)	92.30(15)
Ti(1)−O(4)	2.147(4)	O(13)−Ti(1)−O(3)	97.95(15)
Ti(1)−O(5)	2.042(3)	O(13)−Ti(1)−O(4)	86.82(15)
Ti(1)−O(6)	2.086(3)	O(13)−Ti(1)−O(5)	97.57(15)
Ti(1)−O(13)	1.784(3)	O(13)−Ti(1)−O(6)	93.07(15)
Ti(2)−O(7)	2.004(4)	O(1)−Ti(1)−O(2)	76.67(14)
Ti(2)−O(8)	2.097(3)	O(3)−Ti(1)−O(4)	72.58(14)
Ti(2)−O(9)	2.026(4)	O(5)−Ti(1)−O(6)	73.86(13)
Ti(2)−O(10)	2.153(3)		
Ti(2)−O(11)	2.078(4)		
Ti(2)−O(12)	2.032(3)		
Ti(2)−O(13)	1.822(3)		

oxygen donor at the axial position on the other side. Given the modest quality of the statistics and the similarity of the bond lengths (see below), it is very difficult to discriminate the orientation of the HOPO. This assignment is thus uncertain, but represents the best model to fit the data. As expected, Ti−O distances were shortest to the oxo oxygen (average 1.80 Å) and longer to the HOPO oxygen atoms, with shorter average distances to the NO oxygen donors (2.04 Å) than to the carbonyl oxygen donors (2.09 Å). Ligand bite angles averaged 74.3°, and angles between the oxo oxygen and the other axial ligand were 168.75° and 165.87°. Bond angles between the oxo oxygen and ligand oxygens in the pentagonal plane averaged 93.5°, and between the axial ligand oxygen and the ligand atoms in the plane, 72.18°. Bond angles between the equatorial positions averaged 72°, with one narrower angle (67.37° for O(3)−Ti(1)−O(5) and 68.72° for O(7)−Ti(2)−O(9)) accommodating a rather longer bond from one of the HOPO ligands on each Ti atom (Ti(1)−O(4) and Ti(2)−O(10)).

Discussion

Solid State Structures. For both the alTAM and HOPO ligands, crystallization in the presence of methanol led to methoxide-bearing products because of the strong bonding between alkoxides and Ti(IV).[36] Titanium(IV) powerfully lowers the pK_a of methanol and binds the moiety as the methoxide even at low pH. Complexes with ligand/metal ratios of 2:1 and 3:1 were characterized crystallographically, including 6- and 7-coordinate species.

The complexes of Ti with etTAM and meTAM were synthesized in two ways. One of the syntheses, involving a reaction between $Ti(OEt)_4$ and etTAM, gave crystals of a complex **1** containing one Ti atom coordinated to two TAM ligands and two methoxide ions. The other crystallization in the absence of alkoxide yielded complex **3** for which high resolution X-ray quality crystals were not obtained because of disorder in the solvent of crystallization but for which the connectivity of the ligands to Ti could be confirmed. The structure showed Ti bound to three bidentate ligand molecules. The X-ray crystal structure for the 1:3 Ti/alTAM species was determined for another alTAM, isopropylTAM.[22] Bond distances and bond angles for these structures were similar to those seen in similar previously characterized complexes.[22,32]

The complex **1** showed a very interesting coordination for the two K^+ counterions with one of the potassium ions bound by seven oxygen atoms and the other by six oxygen atoms. The potassium ions are responsible for the formation of the extended network. The intramolecular interaction between the catechol oxygen and the NH proton likely contributes to the stability of complex **1**.

The 1,2-HOPO-containing complex **5** was crystallized from MeOH and **6** from water. These are to our knowledge the first X-ray crystal structures showing coordination of Ti with the hydroxypyridinones. The crystal structure of complex **5** shows Ti(IV) bound by two bidentate 1,2-HOPO ligands along with two methoxide ions, while the structure of complex **6**, prepared in the absence of potential alkoxide ligands, features an oxo-bridged titanium dimer, with each 7-coordinate titanium(IV) ion coordinated by three HOPO ligands. X-ray crystal structures of Ti(IV) complexes having linear hydroxamates were reported by Lippard and Sharpless[35] and by Brown.[36] The former was a Ti dimer with two hydroxamates and two tartrate molecules in the coordination sphere, while the latter bore a mixed hydroxamate/diketonate chelating ligand. The average Ti−O bond lengths for the NO−Ti bond in the complexes with linear hydroxamates (average 1.96 Å for the Lippard complex and 1.95 Å for the Brown complex) are shorter than in complexes **5** (2.01 Å) and **6** (2.04 Å). The Ti−O(C) bond lengths are more similar: 2.08 Å for both complexes of linear hydroxamates and 2.06 Å and 2.09 Å for complexes **5** and **6**, respectively. Thus, for the linear hydroxamates, there is a clear difference between the shorter hydroxmate NO−Ti(IV) distance and the longer hydroxamate CO−Ti(IV) distance, because the hydroxamate oxygen bound to nitrogen formally bears a negative charge and forms shorter bonds to the metal, whereas the one bound to carbon is formally a carbonyl and neutral. In complexes **5** and **6**, with cyclic HOPO ligands facilitating charge delocalization, there is a much smaller difference in those bond distances, primarily because of lengthening of the NO-Ti(IV) bonds. The average O−Ti−O bite angles are similar between the linear hydroxamate (75.5° and 76.2°)[35,36] and HOPO (76.5° and 74.3°) complexes. The previously reported complexes were either

moisture-sensitive or else their aqueous sensitivity was not reported. The present complexes are air and moisture stable. Taken together, the isolation of these HOPO complexes suggests that the HOPO ligands are sufficiently avid to stabilize Ti(IV) with respect to hydrolytic precipitation (with the additional biological implication that HOPOs used for example in chelation therapy may bind Ti(IV) in the body), that alkoxide structures can form when alkoxide ligands are available, and that seven-coordinate structures are accommodated.

The bis-chelating coordination observed in complexes **1** and **5** is a possible model for siderophores and tunichromes with only two sites of chelation. This type of coordination might occur for the siderophore rhodotorulic acid or the tunichrome Mm-1. The latter has been modeled and the structure is shown in Supporting Information, Figure S11. Similar stoichiometry was observed in case of vanadium binding to An-1, a tunichrome from *Ascidia nigra*, even though An-1 possesses three potential sites of chelation.[13] In some cases there may be a steric preference for a 1:2 metal/ligand complex and this coordination may be a typical one observed in nature. The 1:3 coordination observed in complex **3** or **6** serves as a possible model for tris-chelating biomolecules. The oxo-bridged complex **6** suggests that, in the presence of less-donating HOPO ligands as compared to more-donating catechol ligands, hydrolysis of bound water is facilitated, with an oxo-bridged structure crystallized from solution below pH 2.

Similar coordination could also exist on the reaction of hydroxamates with metal oxide surfaces to form self-assembled monolayers[56,57] and on the reaction of siderophores with metal surfaces resulting in the inhibition of bacterial growth.[58,59] This activity of hydroxamates has applications in the prevention of bacterial biofilm formation, which is associated with infections in surgical implants, contamination in food processing environments, and fouling in industrial environments and aquatic ecosystems. Hydroxamates were also used for ore flotation. Titanium oxides, rutile and anatase, are present as a contaminant in ores like kaolinite and feldspar and can be removed by binding to hydroxamate ligands.[60−62]

Aqueous Chemistry. Both of the ligand types reported here, alTAM and HOPO, successfully stabilized Ti(IV) with respect to hydrolytic precipitation in aqueous aerobic solutions over a broad range of pH values. Mass spectrometry of Ti(IV) complexes with both ligand types provided evidence for 2:1 and 3:1 ligand/metal complexes in solution. In agreement with the solid state structures, in the presence of relatively high concentrations of methanol, methoxide complexes were characterized, while for complexes prepared in the absence of methanol, hydrolytic binding of waters was sometimes favored. In general, Ti(IV) competed effectively with protons for ligand binding even at the very lowest pH values; however, ligand was unable to compete for Ti(IV) with hydrolytic binding of water at higher pH values. But still the Ti(IV) was stable to hydrolytic precipitation at micromolar or even millimolar concentrations.

Given the potential biorelevance of coordination by substituted catechols in both siderophores and tunichromes, the speciation of Ti(IV) complexed to etTAM was studied in more detail in aqueous solution. The titration was reversible and reproducible between pH 3 and 10. Below pH 3, it is likely that the neutral and possibly insoluble $Ti(etTAM)_2$ species was forming by analogy to the iron speciation;[20] release of etTAM, which would be doubly protonated at that pH, might also lead to precipitation of the neutral ligand at such low methanol concentrations. Above pH 3, the three metal-containing species best able to fit the data at several metal/ligand ratios were $Ti(etTAM)_3^{2-}$, $Ti(etTAM)_2(OH)_2^{2-}$ (or a species of equivalent degree of hydrolysis, such as $[Ti(etTAM)_2(O)]_2^{4-}$), and a more-hydrolyzed species, modeled here as $Ti(etTAM)(OH)_4^{2-}$. The $Ti(etTAM)_3^{2-}$ species crystallized as complex **3**. The crystallographically characterized complex **1** is similar to $Ti(etTAM)_2(OH)_2^{2-}$, with methoxide ligands (present under the crystallization conditions but not in abundance in the titration) replacing hydroxides. The mass spectrum of complex **1** redissolved in water shows the presence of both 1:2 and 1:3 species in solution, in further support of a speciation scheme like that shown in Figure 5.

The formation constants for Ti(IV) complexes with etTAM ($\log \beta_{130} \geq 55$) are larger than those for the analogous complexes of Fe(III) and Th(IV) with TAM ligands.[20] This trend in the $\log \beta$ values is probably a consequence of the comparable size and greater Lewis acidity of Ti(IV) versus Fe(III) and smaller size of Ti(IV) as compared to Th(IV). Comparing Ti(IV) and Fe(III), the speciation is shifted to lower pH, with the MLH 130 species that forms above pH 8 for Fe(III) predominating by pH 3 for Ti(IV). In addition to the difference in formation constants, the coordination is also different in the case of Th(IV),[21] in that Th(IV) can bind four etTAM molecules whereas Ti(IV) and Fe(III) can only bind a maximum of three. Finally, etTAM, with its electron-withdrawing amide groups, is a less strong ligand than unsubstituted catechol. The β_{130} value estimated between 55 and 60 reflects this fact; it is high enough to allow the complex to predominate at pH 3 but slightly lower than that for Ti(IV) and catechol.[32,55] That the alTAMs are less strong ligands than catechol is also demonstrated at the higher pH region of the titration, where hydrolysis products begin to form at lower pH than for the complexes with catechol.[32]

The coordination and stability of Ti in these complexes gives some idea of the type of potential coordination for Ti in marine organisms. Ascidians like *E. ritteri* that accumulate Ti in high concentrations could make use of this type of coordination to prevent hydrolytic precipitation of titanium. Because Ti(IV) competes with protons for ligand binding even at very low pH, these catecholamides are avid Ti(IV) ligands even at low pH values. Similar properties should be expected for the natural

(56) Folkers, J. P.; Gorman, C. B.; Laibinis, P. E.; Buchholz, S.; Whitesides, G. M.; Nuzzo, R. G. *Langmuir* **1995**, *11*, 813–824.
(57) Lorenz, A.; Kickelbick, G.; Schubert, U. *Chem. Mater.* **1997**, *9*, 2551–2560.
(58) Yang, J.; Bremer, P. J.; Lamont, I. L.; McQuillan, A. J. *Langmuir* **2006**, *22*, 10109–10117.
(59) Upritchard, H. G.; Yang, J.; Bremer, P. J.; Lamont, I. L.; McQuillan, A. J. *Langmuir* **2007**, *23*, 7189–7195.
(60) Celik, M. S.; Can, I.; Eren, R. H. *Miner. Eng.* **1998**, *11*, 1201–1208.
(61) Celik, M. S.; Pehlivanoglu, B.; Aslanbas, A.; Asmatulu, R. *Miner. Metall. Process.* **2001**, *18*, 101–105.
(62) Mathur, S. *J. Colloid Interface Sci.* **2002**, *256*, 153–158.

tunichromes and siderophores, which have similar functionality and additionally are chelating. The pH of the blood of *E. ritteri* is only ~2,[30] but a putative tris-catechol biomolecule might be fully deprotonated and fully tris-chelating even at that very low pH. Also, Ti(IV) might compete with and interfere with Fe(III) biogeochemical or *in vivo* nutrient cycling, when that cycling involves catechol ligands.

The fact that judicious ligand choice can prevent hydrolytic Ti(IV) precipitation even at high micromolar or even millimolar concentrations could be particularly advantageous in medicine. Complexes of Ti(IV) such as titanocene dichloride possess anticancer properties but the precipitation of the complex at neutral pH is blamed for the low efficiency of their anticancer activity.[27−29] Controlled hydrolysis without precipitation may be more advantageous.[63] Details will depend on whether the intact Ti(IV) complex is bioactive, or whether the delivered molecule is effectively a pro-drug, releasing the metal ion to another Ti(IV) binding environment in vivo. The stability constants for the binding of Ti(IV) to etTAM are reasonably high but not as high as Ti(IV) catecholate, and the etTAM ligands afford the possibility of steric tuning by modification of the alkyl groups.

The reduction potential of the Ti(IV)etTAM complex **1** in 20% MeCN/80% H_2O was quite negative (~−0.98 V). This value is slightly less negative than the −1.14 V observed for the Ti tris-catecholate complex,[32] suggesting that etTAM is less stabilizing of the Ti(IV) oxidation state relative to Ti(III). However, it is still low enough that in natural systems at pH 7, similar Ti complexes would not be reduced by any biological reducing agents like NADPH (E^0 = −0.32 V),[64] glutathione (E^0 = −0.23 V),[64] or DTT (E^0 = −0.33 V),[65] unless the equilibrium is driven by a very large excess of the reductant, and will not participate in redox chemistry with the catechol itself, which can be oxidized in certain cases. Hence, the chemistry observed in the case of vanadium in which V(V) is reduced by natural agents to V(IV) and V(III) will not be as likely in case of Ti(IV). In the coordination environments reported here, Ti(III) is not anticipated under the expected environmental or biological conditions. The function (if any) of titanium in ascidians like *E. ritteri* may not include a redox role and thus may be different from the function (still in debate) of vanadium.

(63) Peri, D.; Meker, S.; Shavit, M.; Tshuva, E. Y. *Chem.—Eur. J.* **2009**, *15*, 2403–2415.
(64) Fasman, G. D. *CRC Handbook of Biochemistry and Molecular Biology I*; CRC Press: Cleveland, 1975.
(65) *The Merck Index*; Budvari, S., Ed.; Merck & Co.: Rahway, NJ , 1989; p 3389.

Conclusions

The complexes of Ti with etTAM, meTAM, and 1,2-HOPO were synthesized and studied. Each of these ligands successfully stabilizes Ti(IV) to hydrolytic precipitation over a broad pH range. The complexes of Ti with etTAM were characterized by using X-ray crystallography, mass spectrometry, and cyclic voltammetry. Species having ligand/metal ratios of 3:1 and 2:1, and further hydrolyzed species, occur as a function of ligand and pH. The reduction potential of the complex was highly negative suggesting that biological agents like tunichromes or NADPH would not be able to reduce Ti(IV) to the Ti(III) oxidation state. The pH-dependent speciation of the complex with etTAM in aqueous solution was modeled by using three metal-containing species. The stability constants for these complexes are quite high, indicating strong bonding and suggesting that a similar coordination in nature would lead to the solubilization and perhaps sequestration of Ti. Binding of titanium to siderophores in the environment has been little considered, and in addition, it is possible that ascidians may use this type of coordination in the form of tunichromes to accumulate Ti.

Acknowledgment. We thank Dr. Helmut Ernstberger for his help with cyclic voltammetry and Mr. Justin Presant for help with the HOPO project. Acknowledgement is made to the donors of the Petroleum Research Fund, administered by the American Chemical Society, and the Research Corporation's Research Innovation Award RI0961, for partial support of this research. This research was primarily supported by a American Cancer Society New England Division Research Scholar Grant. We thank the Yale College Dean′s Research Fellowship for funding H.P.I.

Supporting Information Available: The structure of the potassium tetramer from the X-ray crystal structure of complex **1**, intramolecular interaction of the N−H hydrogen and the catecholic oxygen, detailed structure of the 1:3 Ti/etTAM species, ESI-MS of complexes **2**, **3**, **4**, and **5** in solution, cyclic voltammetry of **4**, the cif file for the imperfectly resolved X-ray crystal structure of complex **2** and the cif file for the X-ray crystal structure of complexes **1**, **5**, and **6**. This material is available free of charge via the Internet at http://pubs.acs.org.